Electronic Supplementary Material

From Wheat Bran Derived Carbonaceous Materials to Highly Stretchable and Durable Strain Sensor

Jing Ren, Xuan Du, Wenjun Zhang, and Ming Xu*

State Key Laboratory of Materials Processing and Die & Mould Technology

School of Materials Science and Engineering

Huazhong University of Science and Technology

Wuhan, 430074, China
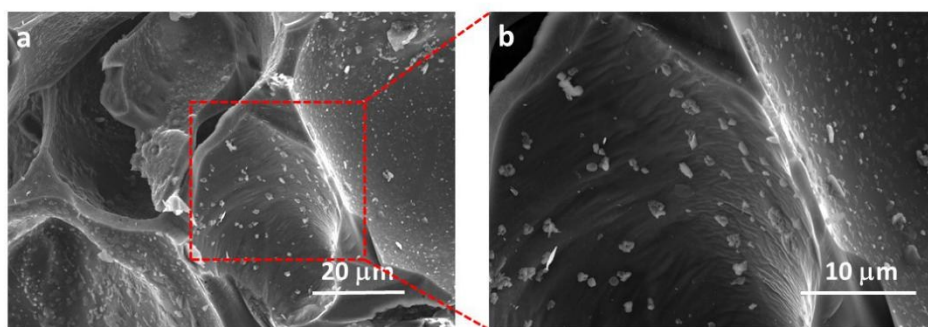
E-mail: ming.xu@hust.edu.cn

Fig. S1. SEM images of carbonized wheat bran processed by high-temperature carbonization (~600 ºC).
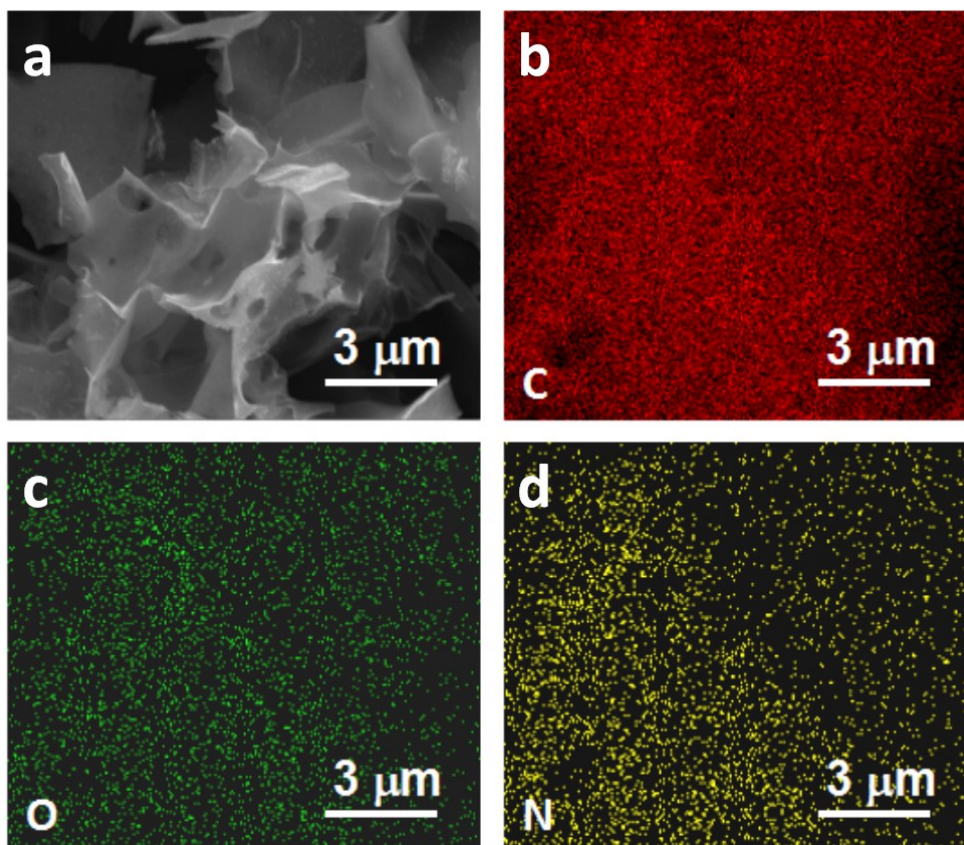
Fig. S2. (a) SEM image of carbon fragments. (b-d) Elements C, O and N mapping of carbon fragments.

The existence and uniform distribution of C, O and N was observed in the surface of carbon fragments, indicating that the N were successfully incorporation onto the carbon fragments through the self-doping process.
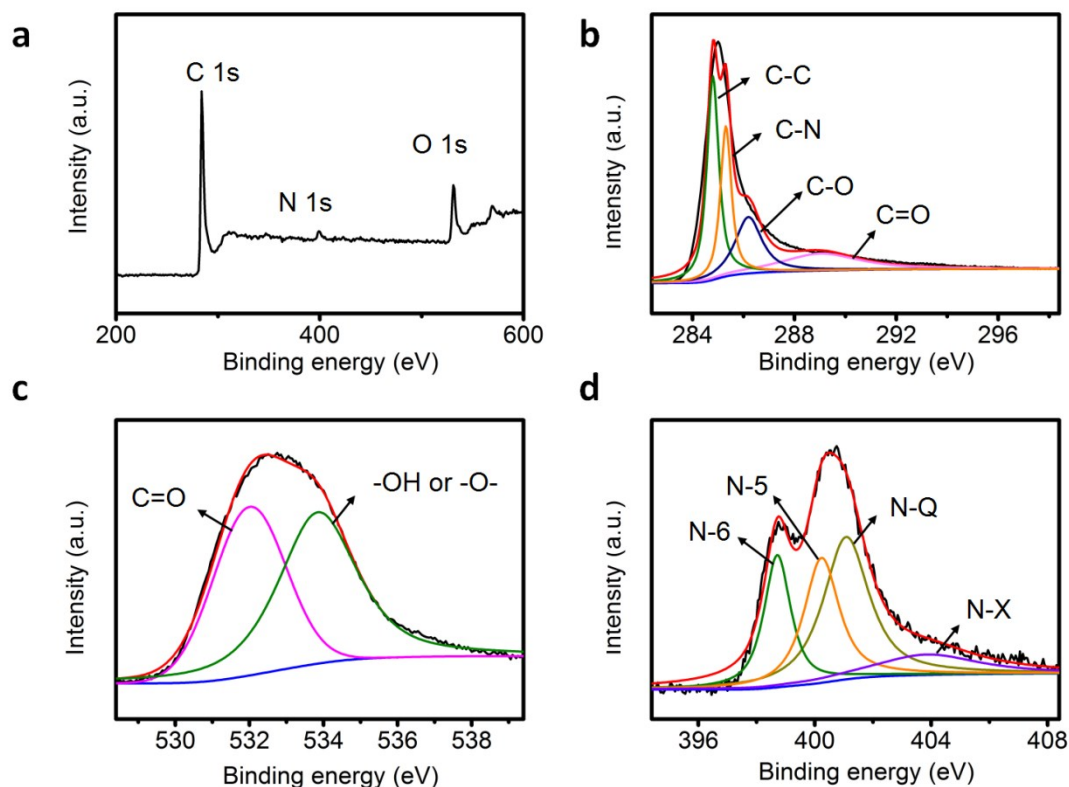
Fig. S3. (a) Wide-scan XPS spectrum and high-resolution XPS spectra of (b) C 1s, (c) O 1s, and (d) N 1s of carbonized wheat bran.

X-ray photoelectron spectroscopy (XPS) measurement was performed to further study the chemical state of the heteroatoms in the carbon fragments. The XPS survey spectra of the carbon fragments confirm the presence of C, O, and N elements. The content of C, O, N in carbon fragments are 82.57 at.%, 12.68 at.% and 4.74 at.%, respectively (Fig. S3a). As shown in Fig. S3b, the high-resolution C1s spectrum is deconvoluted into four individual component peaks, corresponding to C=C (284.8 eV), C-N (285.3 eV), C-O (286.8 eV), and C=O (289.4 eV). Furthermore, the deconvoluted spectra for O1s (Fig. S3c) with two binding energies of 532.0 eV and 533.8 eV are assigned to C=O groups and C-OH groups, respectively. The hydrophilic oxygen-containing functional groups on the surface improved its uniform dispersion in the polar solvent. In addition, the N1s spectrum of the carbon fragments can be fitted

by four peaks: N-6 at 398.7 eV (attributed to pyridinic N), N-5 at 400.2 eV (attributed to pyrrolic N), N-Q at 401.1 eV (attributed to quaternary or graphitic N), and N-X at 403.8 eV (attributed to pyridine-N-oxide N), indicating the transformation of part of N elements within the wheat bran into N functional groups in carbon fragments. The nitrogen-containing functional groups contributes to the good electrical conductivity of the obtained carbon fragments (Fig. S3d).
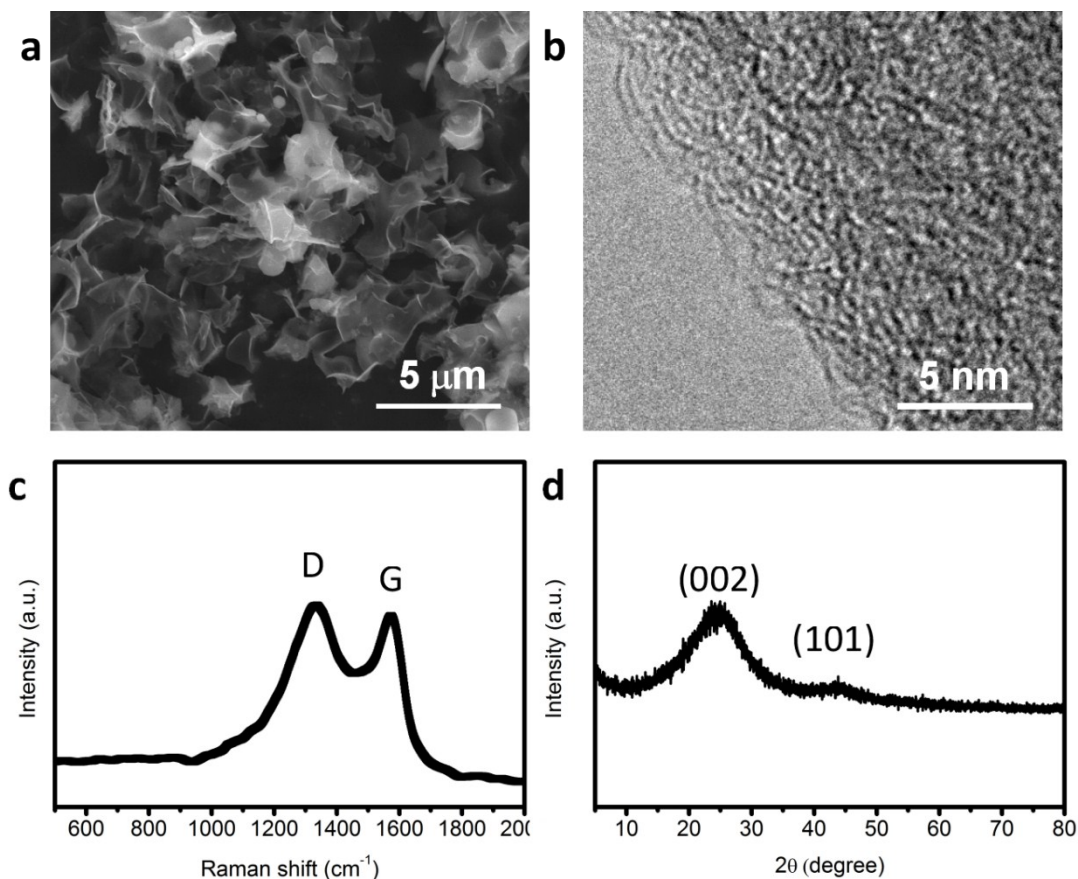
Fig. S4. (a) SEM image of the carbon fragments after KOH activation. (b) High resolution TEM image of the carbon fragments. (c) Raman spectra and (d) XRD pattern of carbon fragments.

The Raman spectrum of the porous carbon presents a G band at 1593 cm^{-1} (associated with crystalline sp^2 carbon) and a D band at 1352 cm^{-1} (related to defects) (Fig. S4c). The intensity ratio (I_G/I_D) can be used to evaluate the degree of graphitic in the carbon samples. The I_G/I_D ratio is calculated to be 0.99 for porous carbon, indicating the characteristic of highly graphitization of carbon materials. The graphitization degree of as-prepared samples was also estimated by the X-ray diffraction (XRD) patterns. As seen in Fig. S4d, the XRD analysis shows two peaks at 26° and 43°, corresponding to the (002) and (101) planes of graphite, indicating the graphitization nature of carbon.
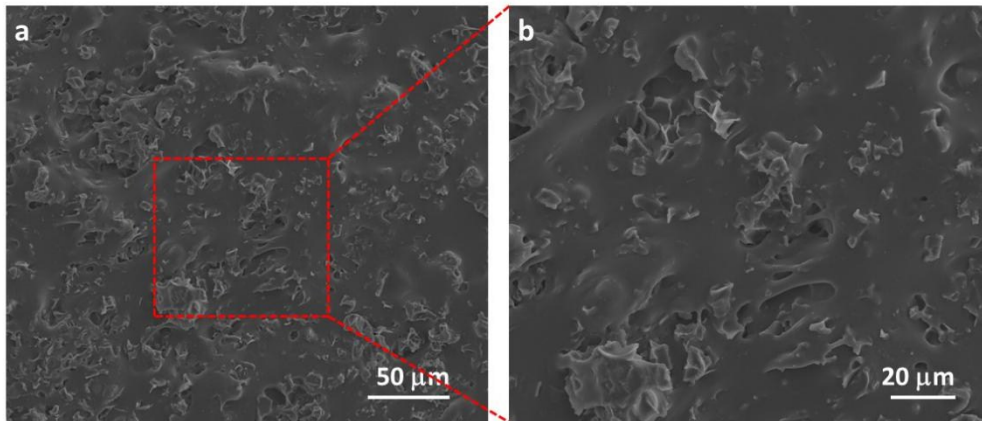
Fig. S5. SEM images of the surface of the strain sensor.

When the strain sensor was peeled off from the glass slide, a few pieces of the carbon fragments on the top surface of the film were exposed to air, which facilitated the electrical wiring process.
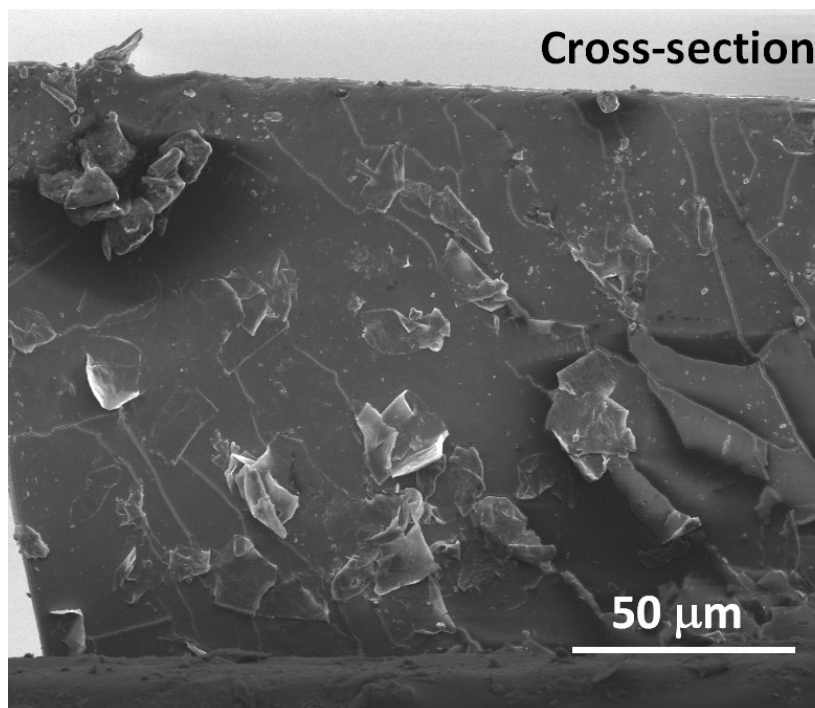

Fig. S6. The SEM image of the cross-section of the strain sensor.

The SEM image of the cross-section of the strain sensor indicated that the carbon fragments could be fully embedded in the PDMS matrix.
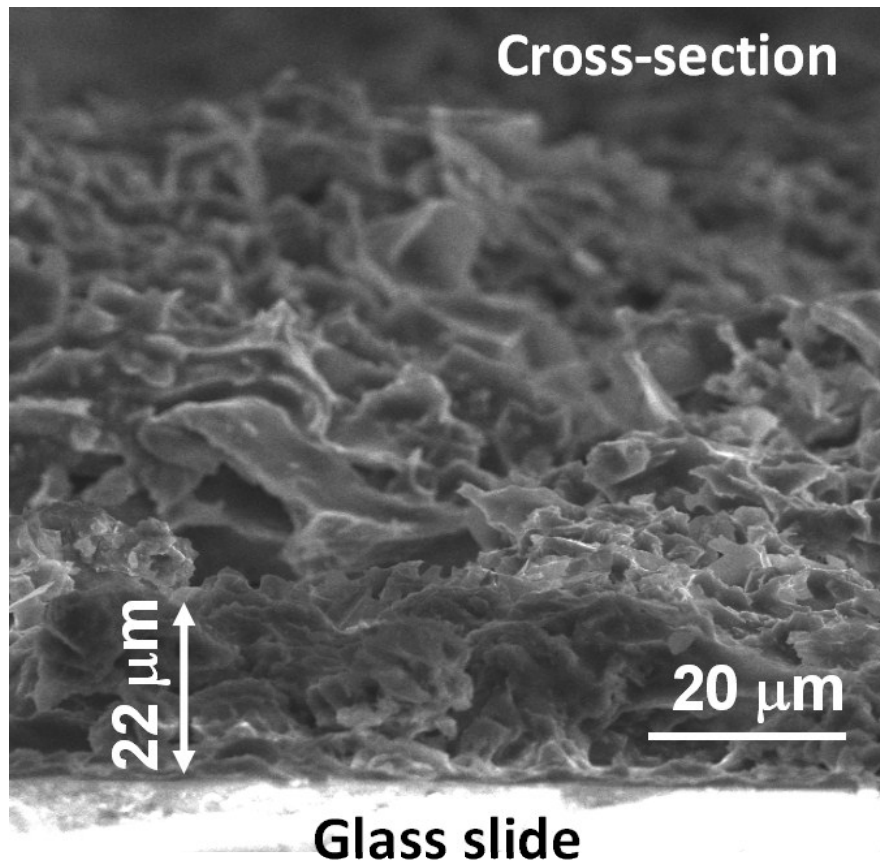

Fig. S7. The SEM image of the cross-section of the carbon fragments film.
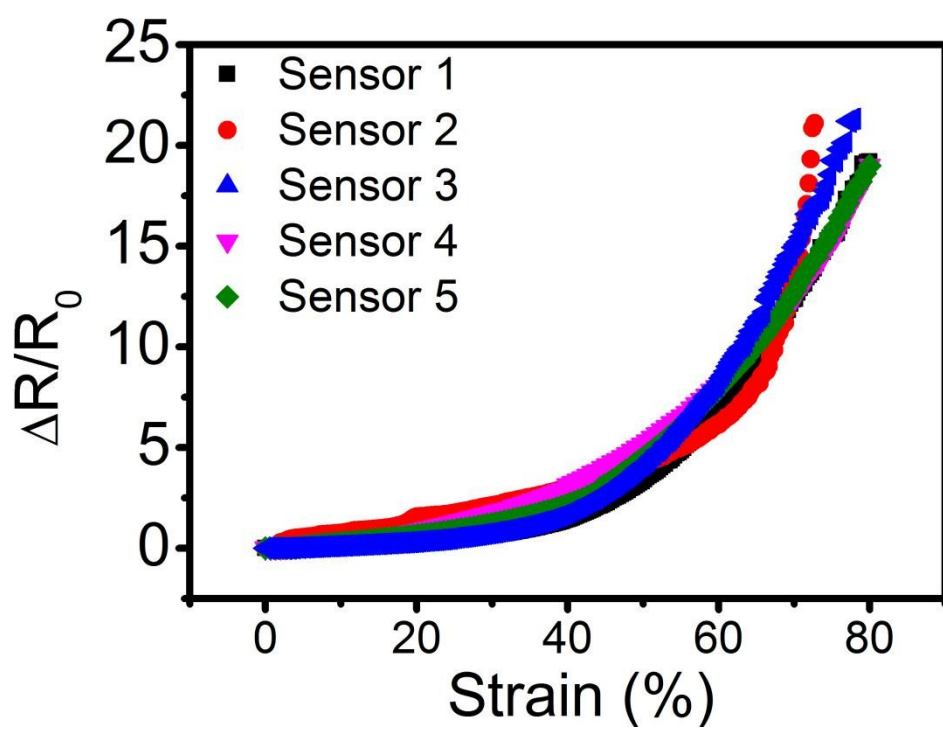
Fig. S8. The relative resistance change of five strain sensors as a function of strain.
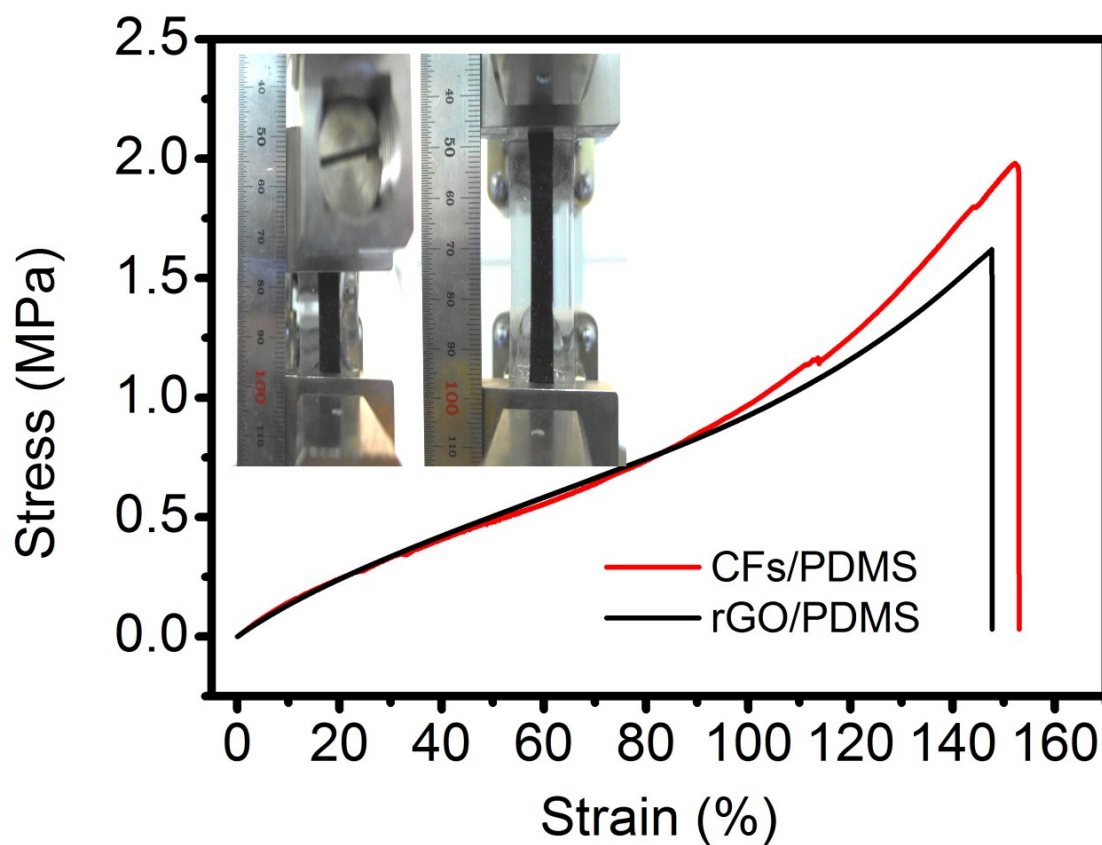
Fig. S9. The tensile stress-strain curves of the two strain sensors. The inset shows the photographs of the CFs/PDMS before and after stretching of ε= 153%.
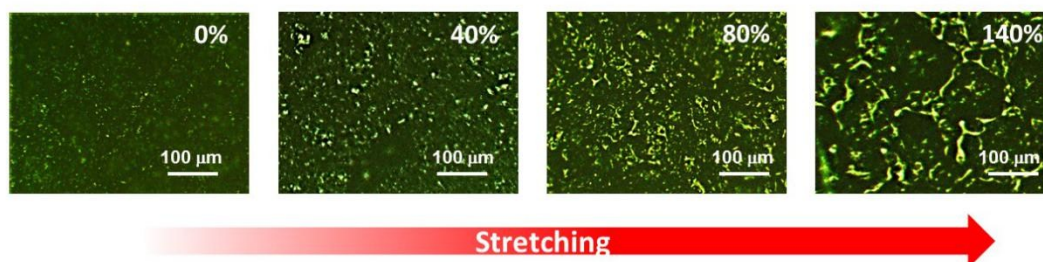
Fig. S10. Optical images of the CFs/PDMS surface morphology at various stretching states.

At 0% strain, the optical images showed the continuous conductive pathways, indicated by the low light transmission. When being stretched to 40% and 80%, the bright spots were gradually produced which were attributed to the separation of neighboring carbon fragments. Finally, these spots were connected to form cracks when being stretched to 140% strain.
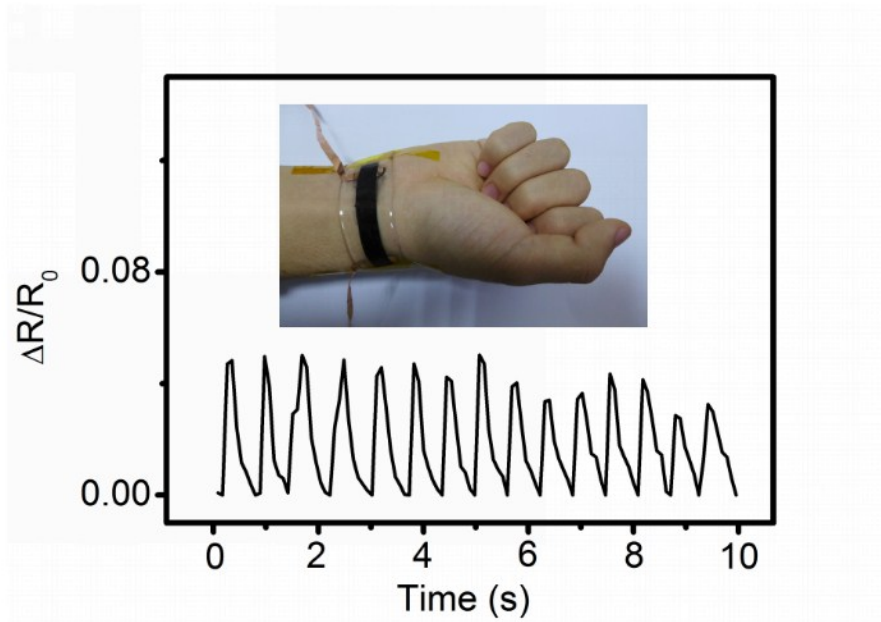
Fig. S11. Demonstration of strain sensor for human movements monitoring. The relative resistance changes of the strain sensor versus time for human wrist pulse detection.

As vital signs, wrist pulse is important to be detected for personal health. The wrist pulse numbers were 15 within 10 s and the data was within the normal range of a healthy adult.

Table S1. Comparison of main performance of the carbon-based stretchable strain sensors.

Raw materials	Strain sensors	Maximum strain	Gauge factor	Durability	Response time and recovery time	Frequency range	Reference
Biomass material	Tissue Paper/PDMS	20%	25.3 (< 3% strain); 9.6 (3%-20% strain);	1,000 cycles at 3% strain	Not shown	0.01-1 Hz at 3% strain	Y. Li *et al.*, *ACS Sustainable Chem. Eng.* 2016. (Ref. 27)
	Carbonized Silk Fabric/Ecoflex	500%	5.8 (< 1% strain); 9.6 (1%-250% strain); 37.5 (250%- 500% strain)	10,000 cycles at 300% strain	response time: 70 ms recovery time: 2 s (100%strain); 6 s (200%strain) ;9 s (300% strain)	0.026-1.25 Hz at 10% strain	C. Wang *et al.*, *Adv. Mater.* 2016. (Ref. 29)
	Carbonized cotton Fabric/Ecoflex	140%	25 (< 80% strain); 64 (80%- 140% strain)	2,000 cycles at 50% strain	Not shown	0.05-0.25 Hz at 50% strain	Y. Zhang *et al.*, *Adv. Funct. Mater.* 2016. (Ref. 28)
Graphene	Fish Scale-Like Graphene/PDMS	82%	16.2 (< 60% strain); 150 (60%-82% strain)	5,000 cycles at 10% strain	Not shown	Not shown	Q. Liu *et al.*, *ACS Nano* 2016. (Ref. 18)
	Graphene/Rubber	800%	35	1,000 cycles at 100% strain	Not shown	Not shown	C. S. Boland *et al.*, *ACS Nano* 2014. (Ref. 19)
	Graphene— Nanocellulose Nanopaper/PDMS	100%	1.6 (10% strain); 7.1 (100% strain)	Not shown	Not shown	Not shown	C. Yan *et al.*, *Adv. Mater.* 2014. (Ref. 15)
	Fragmentized Graphene Foam/PDMS	70%	15-29	10,000 cycles at 50% strain	Not shown	Not shown	Y. R. Jeong *et al.*, *Adv. Funct. Mater.* 2015. (Ref. 20)
Carbon nanotube	Carbon nanotube film/PDMS	280%	0.82 (40% strain); 0.06 (60-200% strain)	10,000 cycles at 200% strain	response time: 14 ms recovery time: 5 s (100% strain)	Not shown	T. Yamada *et al.*, *Nat. Nanotechnol.* 2011. (Ref. 38)
	Carbon nanotube meshes/PDMS	15%	4	1,000 cycles at 20% strain	Not shown	Not shown	F. M. *et al.*, *Nanoscale*, 2016. (Ref. 13)
Carbon black	Carbon black/ Thermoplastic elastomer	100%	20	3,800 cycles at 80% strain	recovery time: 100 s (100% strain)	Not shown	C. Mattmann *et al.* *Sensors*, 2008 (Ref. 39)
Biomass material	Carbon Fragments Derived from Wheat Bran/PDMS	153%	2.2 (<40% strain); 62.8(40%-80% strain)	10,000 cycles at 80% strain	response time: ~60 ms recovery time: 3 s (40% strain); 7 s (60% strain) ; 10 s (80% strain)	0.01-1 Hz at 80% strain	Our work